Tohoku J. Exp. Med., 2019, **249**, 43-56

LncRNA SNHG3 Promotes Hepatocellular Tumorigenesis by Targeting miR-326

Qian Zhao,[1] Chensi Wu,[1] Jingwen Wang,[1] Xidong Li,[1] Yuchen Fan,[1,2] Shuai Gao[1,2] and Kai Wang[1,2]

[1]Department of Hepatology, Qilu Hospital of Shandong University, Jinan, Shandong, China
[2]Institute of Hepatology, Shandong University, Jinan, Shandong, China

Small nucleolar RNA host gene 3 (SNHG3), a long noncoding RNA (lncRNA), acts as an oncogene in hepatocellular carcinoma (HCC), whereas microRNA (miR)-326 plays an inhibitory role in some types of human cancers, including melanoma, osteosarcoma, and gastric cancer. In the present study, by analyzing 47 tissue specimens of human HCC, we found that the relative expression levels of SNHG3 were significantly higher in HCC tissues than those in the adjacent noncancerous tissues, whereas the relative expression levels of miR-326 were significantly lower in HCC tissues. Furthermore, the relative mRNA levels of Sma and Mad Related Family 3 (SMAD3) and zinc finger E-box binding homeobox 1 (ZEB1) were significantly higher in HCC tissues compared with the adjacent noncancerous tissues. In human HCC cell lines, SNHG3 overexpression promoted the proliferation, migration, and epithelial-mesenchymal transition and inhibited apoptosis, whereas knockdown of SNHG3 expression exerted the opposite effects. Importantly, miR-326 or miR-326 inhibitor restored the aforementioned effects of SNHG3 overexpression or SNHG3 knockdown. We thus found that the miR-326-response element is present in SNHG3 and the 3'-untranslated region of SMAD3 mRNA. In fact, SNHG3 overexpression increased the expression levels of SMAD3 and ZEB1, while miR-326 decreased the expression levels of SMAD3. These results suggest that SNHG3 may function as a competing endogenous RNA (ceRNA) for miR-326, which in turn enhances SMAD3 and ZEB1 expression. In conclusion, we propose that SNHG3 promotes HCC progression via the miR-326/SMAD3/ZEB1 signaling pathway. The findings may provide novel targets for the diagnosis and treatment of HCC.

Keywords: hepatocellular carcinoma; long noncoding RNA; miR-326; Sma and Mad Related Family 3; zinc finger E-box binding homeobox 1
Tohoku J. Exp. Med., 2019 September, **249** (1), 43-56. © 2019 Tohoku University Medical Press

Introduction

With approximately 600,000 new cases annually, hepatocellular carcinoma (HCC) is one of the most common malignancies and leading cause of cancer-related deaths worldwide (Forner et al. 2012; Torre et al. 2015). Most patients are diagnosed at advanced stages without the opportunity for curative surgical resection; thus, the mortality of HCC is high (Wen et al. 2018). Despite the rapid development in treatment strategies, including systemic chemotherapy, transcatheter arterial chemoembolization, and radiofrequency ablation, the outcomes of advanced patients with HCC remain unsatisfactory (Maluccio and Covey 2012). It is therefore necessary to elucidate the detailed molecular bases involved in HCC progression and explore new therapeutic strategies to improve the prognosis of patients with HCC.

Long noncoding RNA (lncRNA) refers to a family of RNAs greater than 200 nt in length but is not translated into protein (Nagano and Fraser 2011). LncRNAs possess significant biological functions in tumor progression, including epithelial-mesenchymal transition (EMT), invasion-metastasis, proliferation, apoptosis, and drug resistance (Ponting et al. 2009; Esteller 2011). Dysregulated lncRNAs might act as oncogenes or tumor suppressors during HCC progression (Wang et al. 2014a; Yuan et al. 2014; Ge et al. 2015; Wang et al. 2015). For instance, pituitary tumor-transforming 3, pseudogene (PTTG3P), a lncRNA, promoted the proliferation and metastasis of HCC by activating PTTG1 and the phosphatidylinositol-3-kinases/protein-serine-threonine kinase (PI3K/AKT) pathway (Huang et al. 2018). Noncoding repressor of NFAT (NRON), a newly identified repressor of nuclear factor of activated T cells (NFAT), suppresses HCC growth and metastasis through

Received March 12, 2019; revised and accepted September 9, 2019. Published online September 21, 2019; doi: 10.1620/tjem.249.43.
Correspondence: Kai Wang, M.D., Ph.D., Department of Hepatology, Qilu Hospital of Shandong University and Institute of Hepatology, Shandong University, 107# Wenhuaxi Road, Jinan, Shandong 250012, China.
e-mail: wangdoc876@126.com; wangdoc2010@163.com

inhibiting EMT (Yao et al. 2018). However, the functions of many lncRNAs remain unclear.

Small nucleolar RNA host gene 3 (SNHG3; GenBank accession no. NR_036473.1), located on 1q35.3, is a lncRNA discovered by Pelczar and Filipowicz (1998). SNHG3 is involved in various functional regulations. SNHG3 regulated mouse embryonic stem cell self-renewal and pluripotency (Lu et al. 2019). Moreover, the research on SNHG3 has investigated the function on tumorigenesis of certain cancers. SNHG3 promoted malignant development of colorectal cancer (Huang et al. 2017b). Increased expression of SNHG3 was associated with poor prognosis and enhanced malignant progression of ovarian cancer (Hong et al. 2018), lung adenocarcinoma (Liu et al. 2018), and glioma (Fei et al. 2018). In addition, data mining of the Cancer Genome Atlas and Oncomine databases indicated that increased SNHG3 expression was correlated with the malignant status and poor prognosis of patients with HCC (Zhang et al. 2016; Zhang et al. 2019). Nonetheless, the association of SNHG3 with the incidence and tumorigenesis of HCC remain unknown and should be addressed in further investigations.

LncRNAs were observed to regulate mRNA expression as competitive endogenous RNAs (ceRNAs) of microRNAs (miRNAs) after transcription (Salmena et al. 2011). For instance, X-inactive specific transcript (XIST) could regulate the expression of gene of phosphate and tension homology deleted on the chromosome ten (PTEN) by inhibiting miR-181a in the progression of HCC (Chang et al. 2017), and linc00673 promoted the occurrence of non-small cell lung cancer through regulating zinc finger E-box binding homeobox 1 (ZEB1) by interacting with miR-150-5p (Lu et al. 2017). ZEB1 promoted invasion and metastasis in several types of human cancer and had a prognostic role in certain cancers (Lazarova and Bordonaro 2017). Additionally, ZEB1 was transcriptionally activated by SMAD3 in HCC and promoted tumorigenesis (Ahn et al. 2012).

MiRNAs, the same as lncRNAs, have long been widely recognized in malignancies. MiR-326 acted as a tumor suppressor in several malignancies and targeted different genes in glioma, endometrial cancer, and cervical cancer (Li et al. 2015b; Wu et al. 2017; Zhang et al. 2017; Yin et al. 2018). However, no studies have reported the interaction between SNHG3 and miR-326 in HCC.

In this study, we hypothesized that SNHG3 might promote HCC progression by targeting miR-326 expression. The expression levels of SNHG3 and miR-326 in HCC tissues and paracancerous tissues were measured first. Then the potential functions of SNHG3 and its relationship with miR-326 were explored *in vitro* and *in vivo*. The results of this study may contribute to the discovery of new therapeutic targets for HCC.

Materials and Methods

Ethics statement and tissue specimens

Informed consent was obtained from all patients. All experiments in humans and animals were approved by the Institutional Review Board of Qilu hospital. All experiments were performed in accordance with the approved guidelines and regulations, including any relevant details. 47 pairs of HCC tissues and matched adjacent noncancerous tissues were obtained from Qilu Hospital of Shandong University. Each sample was rapidly frozen in liquid nitrogen and stored at −80°C. The patients' clinical characteristics are listed, without any information that could identify patients (see Table 1).

Cell lines and cell culture

Human HCC cell lines (HepG2 and HCCLM3) and the normal hepatocyte (L02) were purchased from the Chinese Academy of Sciences Cell Bank (Shanghai, China). All cells were routinely cultured in Dulbecco's Modified Eagle Medium (DMEM, HyClone, USA) supplemented with 10% fetal bovine serum (FBS, HyClone, USA), and penicillin and streptomycin (100 units/ml, Gibco, USA) at 37°C under 5% CO_2.

Quantitative reverse transcription-polymerase chain reaction (qRT-PCR)

Total RNA was extracted from human HCC tissues and cells with Trizol (Invitrogen, USA). qRT-PCR for mRNA and lncRNA was performed with a HiScript 1st Strand cDNA Synthesis Kit and SYBR Green I Real-Time PCR Kit (Vazyme Biotech Co. Ltd, China) according to the manufacturer's instructions. qRT-PCR for miRNA was performed with a miScript II RT Kit and miScript SYBR Green PCR Kit (Qiagen, Germany) according to the manufacturer's instructions. Quantitative PCR was performed using a Bio-Rad CFX-96 detection system (Bio-Rad, USA). The relative expression levels of miRNA, mRNA and lncRNA were normalized to those of U6 and β-actin. Primers were supplied by Qiagen.

Cell transfection

For changing the expression levels of miR-326 in HCC cells, miR-326 mimic, and miR-326 inhibitor (anti-326), and the corresponding negative control (NC-mimic and anti-NC) were synthesized and purified by Sangon (Shanghai, China). To reduce expression levels of SNHG3 or ZEB1 in HCC cells, the small interfering RNA (siRNA) specifically targeting SNHG3 (si-SNHG3) or ZEB1 si-ZEB1 and matched negative control (si-NC) were purchased from Sangon (Shanghai, China). Transfection was performed using Lipofectamine 2000 (Invitrogen Inc., Carlsbad, CA, USA) according to the manufacturer's instruction, and subsequent experiments were performed after 48 hours. Lentiviral vector overexpressing SNHG3 (pLVX-SNHG3) or ZEB1 (pLVX-ZEB1) and the corresponding negative control (pLVX) were purchased from Sigma (Sino Biological, China), and transfections were performed using the recombinant lentivirus-transducing units plus 8 mg/ml polybrene. Three days later, the cells transfected with the lentivirus were subjected to FACS analysis for GFP to obtain the cells stably overexpressing SNHG3 or ZEB1. Then, these cells were transfected with miR-326 mimic or NC mimic. Transfection was performed using Lipofectamine 2000 (Invitrogen Inc., Carlsbad, CA, USA) according to the manufacturer's instruction, and subsequent experiments were performed after 48 hours.

Dual-luciferase reporter assay

A potential miR-326-binding sequence is present in SNHG3 and in the 3′-untranslated region (3′-UTR) of human SMAD3 mRNA. Thus, the respective region containing the complementary sequence to miR-326 was amplified and ligated to the dual-luciferase vector (Promega, USA). Each mutant construct was also generated using Quik Change II Site-Directed Mutagenesis Kit (Agilent Technologies, USA). Cells were transfected with a luciferase vector containing the wild-type miR-326-binding sequence of SNHG3 (SNHG3-WT) or its mutated sequence (SNHG3-MUT) together with miR-326 mimic or NC-mimic using Lipofectamine 2000 according to the manufacturer's instructions. Likewise, cells were transfected with a luciferase vector containing the wild-type 3′-UTR of SMAD3 mRNA (SMAD3-WT) or its mutated 3′-UTR (SMAD3-MUT) together with miR-326 mimic or NC-mimic. Luciferase activity was measured using the Dual-Luciferase Reporter Assay System (Promega, USA) and normalized to that of Renilla luciferase.

Cell viability assay

The viability of transfected HCC cells was determined by the MTT assay. Cells were seeded in 96-well plates at a density of approximately 5×10^3 cells per well. MTT (5 mg/ml) was added to each well for 4 hours after treatment, and then DMSO was added to stop the reaction. Optical density at 490 nm was measured using an Agilent Cary Eclipse (Agilent, USA) and subtracted from the absorbance of the medium. All samples were measured three times, and the mean of each experiment was calculated.

Transwell assay

Transfected cells of each group (approximately 1.5×10^4) were seeded into transwell chambers (8 μm, Corning, USA). The upper chambers were coated with or without 10 μg/ml Matrigel and filled with cells in serum-free media. Media containing 10% FBS was added into the lower chambers. After 48 hours of incubation, the cells in the lower chamber membrane were fixed with 4% polyoxymethylene and stained with 0.1% crystal violet. At least 6 fields were selected; next, migrated cells were photographed and counted under a microscope.

Apoptosis assay

After collected and resuspended in binding buffer, the treated HCC cells were double stained with FTTC-Annexin V and propidium iodide using an Annexin V-fluorescein isothiocyanate (FITC) Apoptosis Kit (Beyotime, Jiangsu, China) according to the manufacturer's instructions and then analyzed using flow cytometry (FACS Calibur, Bio-Rad Laboratories, Inc. USA).

Western blot analysis

HCC cells were collected and lysed with SDS lysis buffer (Sigma, USA), and protein lysates (30 μg) were separated by 10% sodium dodecyl sulfate-polyacrylamide gel electrophoresis (SDS-PAGE) and transferred to polyvinylidene difluoride (PVDF) membranes (Roche, Switzerland). After being blocked with 5% skim milk for 1 hour at room temperature, the PVDF membranes were incubated with primary antibody for 12 hours at 4°C. The main biomarkers for EMT are Vimentin, E-cadherin, and Snail. Primary antibodies against Vimentin, E-cadherin, Snail, SMAD3, ZEB1, and glyceraldehyde-3-phosphate dehydrogenase (GAPDH) and secondary antibodies were purchased from Cell Signaling Technology (CST, USA) and diluted at 1 : 2,000 for use. The final signal was visualized using HRP.

Tumor formation in mice

Twelve female BALB/c nude mice (4-6 weeks old) were used to establish mice xenograft models (n = 6 each group). After transfecting HepG2 cells with si-NC or si-SNHG3, approximately 5×10^6 cells of the aforementioned 2 groups were suspended in 100 μl physiological saline and injected subcutaneously on the right side of the back. Tumor volume (V) was measured with callipers every 3 days and calculated as $V = A \times B^2/2$ (mm^3). Here, A referred to the largest diameter, and B indicated the shortest diameter (Huang et al. 2017a; Huang et al. 2019). Thirty-three days after injection, mice were sacrificed with 1% pentobarbital sodium (Sigma, USA) followed by decapitation, and the tumors were excised. Animal studies were performed in accordance with the guidelines of Qilu Hospital of Shandong University.

HE staining and Ki-67 immunostaining

The subcutaneous tumor tissues of transplanted HCC cells were collected and fixed in 10% formaldehyde, embedded in paraffin, and then sectioned. Ki-67 was used for immunohistochemical analysis, the slides were counterstained with hematoxylin dehydrated and fixed, and sealed with the neutral gum. The results were observed under microscope (Olympus, Japan).

TUNEL assay

The apoptosis levels in the subcutaneously transplanted HCC cells were measured by TdT-mediated dUTP Nick-End Labeling (TUNEL) using a TUNEL kit (Roche TMR-RED, Switzerland) according to the manufacturer's instructions.

Statistical analysis

Data were obtained from 3 independent experiments and presented as the mean ± S.D. SPSS 16.0 software was used for statistical analyses. Intergroup comparisons were verified by Student's t tests. Multiple comparisons were analyzed by one-way analysis of variance, and Pearson correlation analyses were performed. All statistical tests were two-sided, and a P value < 0.05 was considered statistically significant.

Results

Higher SNHG3 levels and lower miR-326 levels in HCC tissues

The expression levels of SNHG3 and miR-326 in 47 pairs of HCC tissues and adjacent noncancerous tissues (as normal controls, NCs) were analyzed using qRT-PCR. The results revealed that SNHG3 levels were significantly higher and miR-326 levels were lower in HCC tissues compared with NCs (Fig. 1A, B). Further analysis indicated the expression trend of SNHG3 in 47 pairs of tissues was opposite to that of miR-326 (Fig. 1C). Patient characteristics including tumor stage, lymph node metastasis, and distant metastasis are summarized in Table 1. The relative expression levels of SNHG3 were closely correlated with TNM stage (Table 1). Moreover, compared with normal hepatocyte (L02), the relative expression levels of SNHG3 were higher in HCCLM3 and HepG2 cells (Fig. 1D), and miR-326 levels were lower in HCCLM3 and HepG2 cells (Fig.

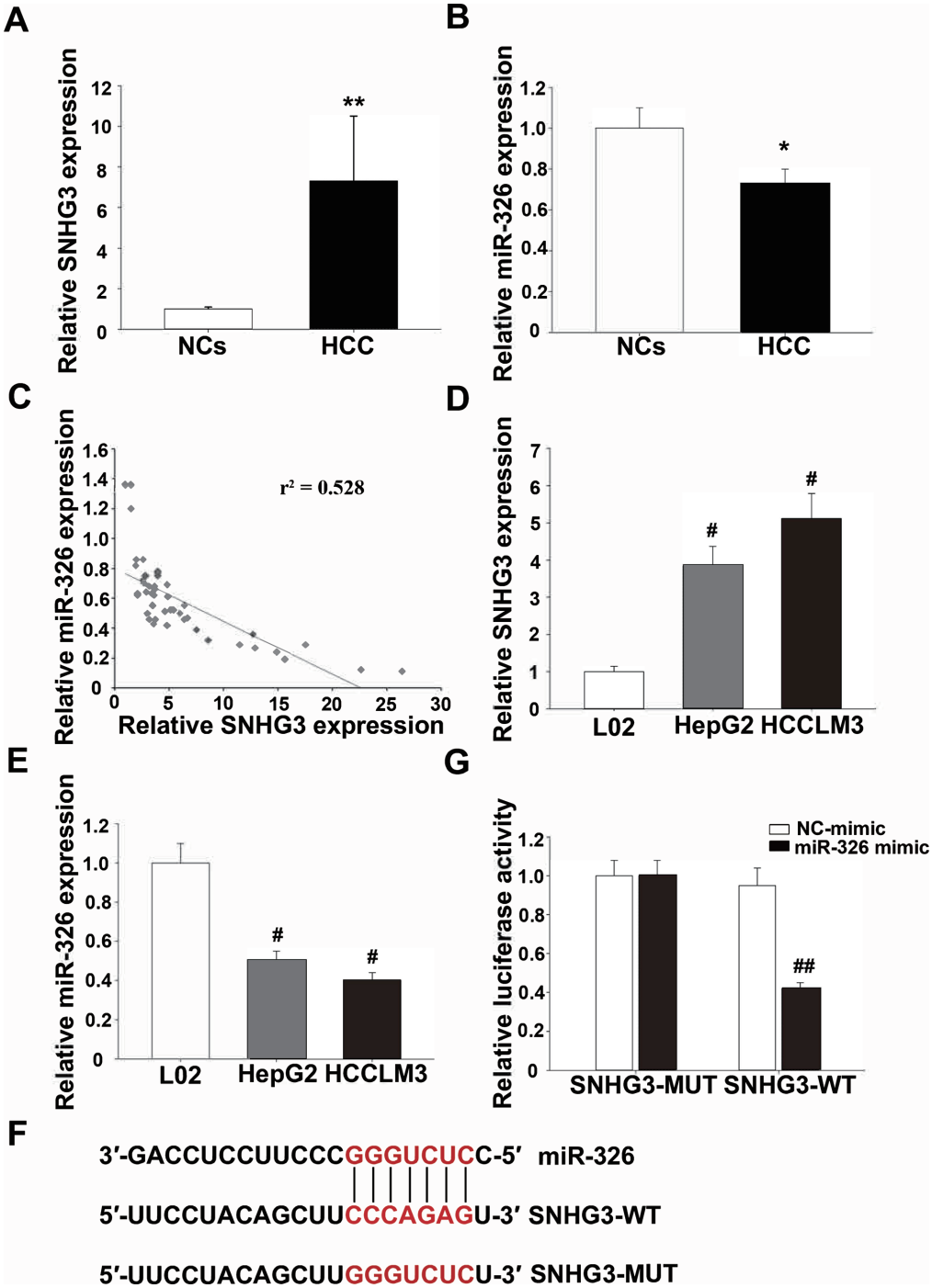

Fig. 1. Relative expression levels of SNHG3 and miR-326 in hepatocellular carcinoma tissues and cell lines.

(A, B) Relative expression levels of SNHG3 and miR-326 in HCC tissues (N = 47) and corresponding adjacent noncancerous tissues, determined by qRT-PCR. Data represent mean ± SD.

*$P < 0.05$; **$P < 0.01$.

(C) Relationship between SNHG3 and miR-326 in 47 HCC tissues. The data were analyzed by Pearson correlation analysis.

(D, E) Relative expression levels of SNHG3 and miR-326 in HCC cells (HCCLM3 and HepG2) and normal liver cells (L02), measured by qRT-PCR. Experiments were repeated at least 3 times; data represent mean ± SD.

$^{\#}P < 0.01$, vs. L02.

(F) Predicted miR-326-binding sequence of SNHG3 (SNHG3-WT: SNHG3 wild type) and its mutant type (SNHG3-MUT).

(G) Luciferase activity in HepG2 cells cotransfected with mi-R326 mimic or NC mimic and the luciferase vector containing sequence of SNHG3 wild type or mutant type. Experiments were repeated at least 3 times; data represent mean ± SD.

$^{\#\#}P < 0.01$, vs. NC mimic.

Table 1. Correlation between SNHG3 expression and patient characteristics.

Characteristic	Number (%)	Relative expression levels of SNHG3	*P* value
Age			0.497
≤ 60	26 (55.3)	6.75 ± 3.79	
> 60	21 (44.7)	7.26 ± 4.67	
Sex			0.595
Male	31 (66.0)	7.36 ± 4.83	
Female	16 (34.0)	6.65 ± 3.69	
Tumor stage			< 0.001
T1	19 (40.4)	5.92 ± 3.29	
T2	13 (27.7)	7.68 ± 4.92	
T3	9 (19.1)	9.69 ± 4.69	
T4	6 (12.8)	13.49 ± 5.61	
Lymph node metastasis			< 0.001
N0	30 (63.8)	5.23 ± 3.29	
N1	17 (36.2)	13.54 ± 5.76	
Distant metastasis			< 0.001
M0	33 (70.2)	6.19 ± 4.19	
M1	14 (29.8)	15.29 ± 7.29	

Data are expressed as the number (percentage) and mean ± SD.

1E). Because the expression level of SNHG3 was marginally lower in HepG2 cells than in HCCLM3 cells, in the subsequent experiments, SNHG3 was overexpressed in HepG2 cells and silenced in HCCLM3 cells, unless otherwise stated.

SNHG3 binds to miR-326

To investigate the functional relationship between SNHG3 and miR-326, we performed bioinformatics analysis using miRcode, showing that SNHG3 contains the potential binding sequence for miR-326 (Fig. 1F). To validate the interaction between SNHG3 and miR-326, we used a luciferase reporter vector containing a miR-326-binding sequence of SNHG3 (SNHG3-WT) or its mutated binding sequence (SNHG3-MUT). In Fig. 1G, luciferase activities were significantly lower in HepG2 cells cotransfected with SNHG3-WT and miR-326 mimic than those in cells cotransfected with SNHG3-WT and NC-mimic, but the luciferase activities were not altered with the mutant SNHG3 vector. These results suggest that miR-326 may bind to the target sequence of SNHG3.

SNHG3 regulates HCC proliferation, migration, apoptosis, and EMT by interacting with miR-326

We then investigated the role of the interaction between SNHG3 and miR-326 in HCC proliferation. Overexpression of SNHG3 significantly increased proliferation and migration abilities of HepG2 cells (Fig. 2A, B), but these enhancing effects of SNHG3 were not detected in cells cotransfected with miR-326 mimic. By contrast, overexpression of SNHG3 significantly decreased apoptosis (Fig. 2C, D), while miR-326 mimic restored the degree of apoptosis. We next performed the knockdown experiments in HCCLM3 cells. SNHG3 depletion with si-SNHG3 significantly reduced proliferation and migration abilities of HCCLM3 cells (Fig. 3A, B) and conversely increased apoptosis (Fig. 3C, D), while these effects were abolished by anti-326 (Fig. 3). Taken together, these data indicate that SNHG3 regulates proliferation, migration, and apoptosis of HCC cells by interacting with miR-326.

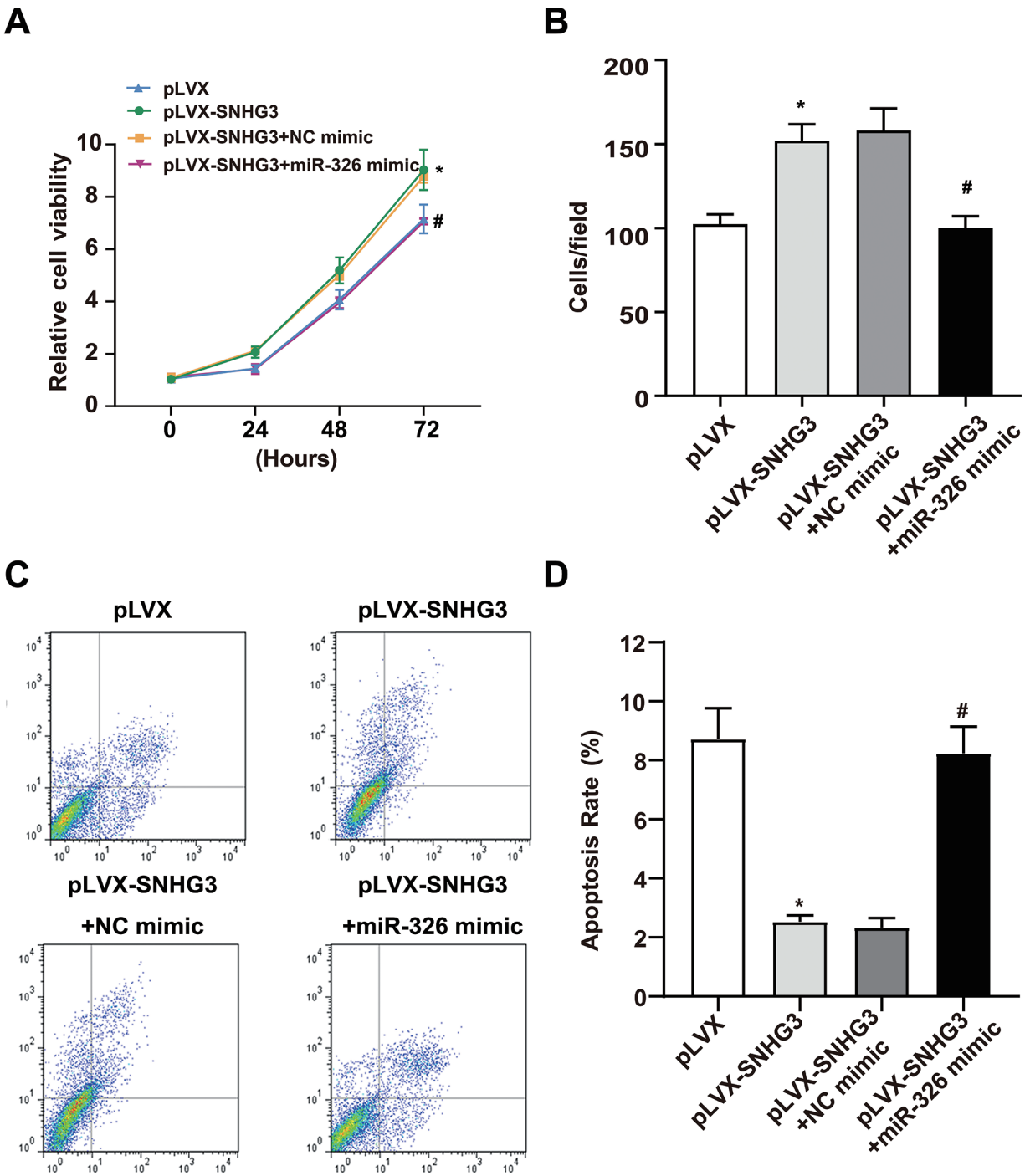

Fig. 2. SNHG3 overexpression promotes HCC proliferation, migration, and inhibits apoptosis by interacting with miR-326. HepG2 cells were transfected with pLVX, pLVX-SNHG3 or cotransfected with pLVX-SNHG3 and miR-326 mimic or NC mimic. Experiments were repeated at least 3 times; data represent mean ± SD.

(A) Enhanced effects of SNHG3 on cell viability. pLVX-SNHG3 enhanced cell viability and miR-326 mimic reversed the enhanced effect of pLVX-SNHG3 on cell viability, judged by MTT assays.

*$P < 0.01$, vs. pLVX; $^{\#}P < 0.01$, vs. pLVX-SNHG3+NC mimic.

(B) Enhanced effects of SNHG3 on cell migration. Transwell assays showed that SNHG3 enhanced cell migration and miR-326 mimic resumed the increased migration ability.

*$P < 0.01$, vs. pLVX; $^{\#}P < 0.01$, vs. pLVX-SNHG3+NC mimic.

(C, D) Suppressive effects of SNHG3 on apoptosis. Flow cytometry showed miR-326 mimic restored the suppressed apoptosis.

*$P < 0.01$, vs. pLVX; $^{\#}P < 0.01$, vs. pLVX-SNHG3+NC mimic.

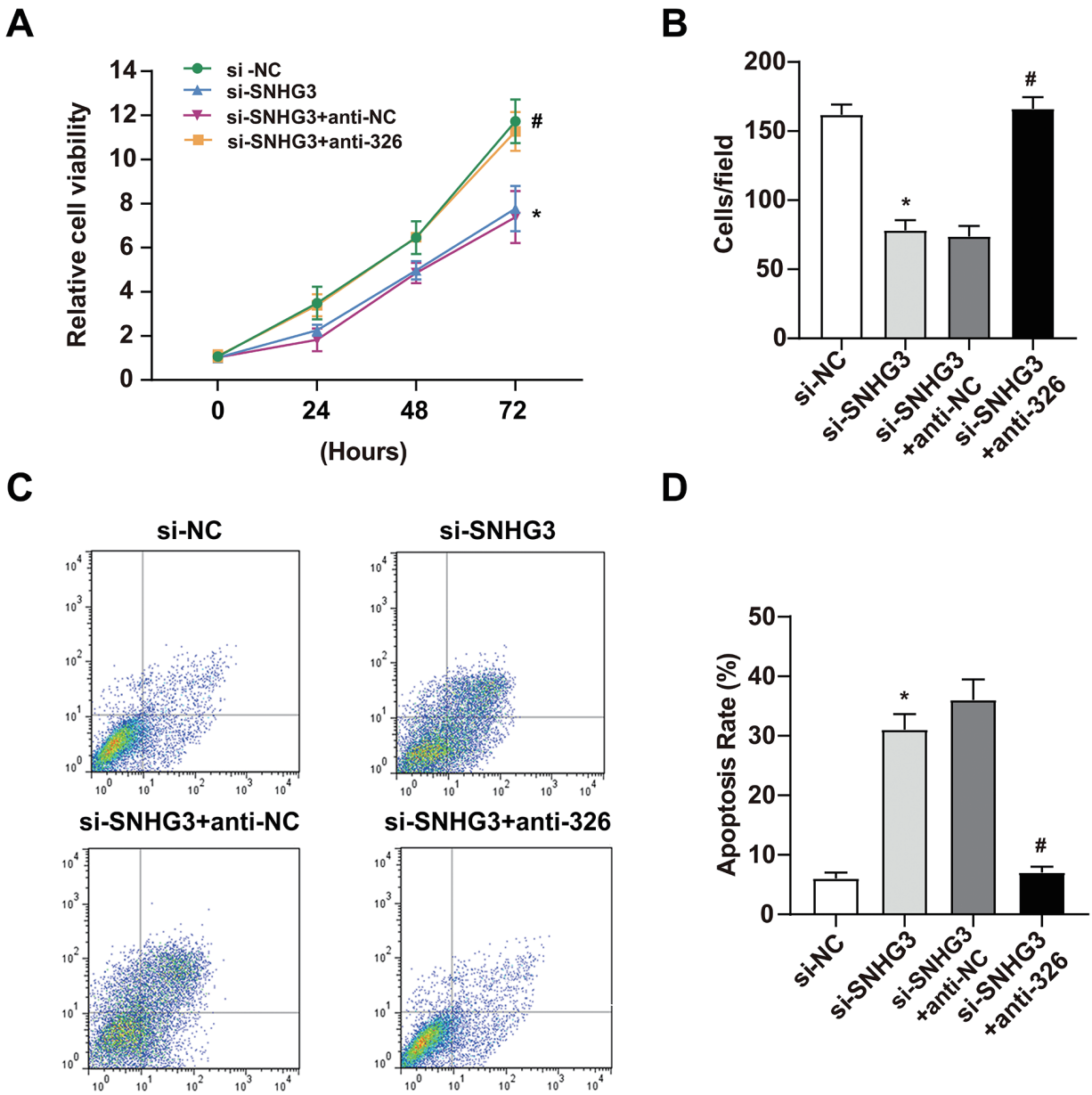

Fig. 3. SNHG3 knockdown suppresses HCC proliferation, migration, and promotes apoptosis by interacting with miR-326. HCCLM3 cells were transfected si-NC, si-SNHG3, or cotransfected with si-SNHG3 and anti-326 or anti-NC. Experiments were repeated at least 3 times; data represent mean ± SD.
(A) MTT assay showed anti-326 resumed decreased cell viability.
*$P < 0.01$, vs. si-NC; $^{\#}P < 0.01$, vs. si-SNHG3+anti-NC.
(B) Transwell assays showed anti-326 resumed decreased migration ability.
*$P < 0.01$ vs. si-NC; $^{\#}P < 0.01$, vs. si-SNHG3+anti-NC.
(C, D) Flow cytometry showed anti-326 restored promoted apoptosis.
*$P < 0.01$, vs. si-NC; $^{\#}P < 0.01$, vs. si-SNHG3+anti-NC.

We also analyzed the roles of SNHG3 and miR-326 in EMT. Overexpression of SNHG3 significantly increased the expression levels of Vimentin and Snail but decreased the expression levels of E-cadherin in HepG2 cells, while miR-326 mimic restored the aforementioned effects (Fig. 4A, B). Knockdown of SNHG3 expression caused the opposite effects in HCCLM3 cells, while anti-326 could resume them (Fig. 4C, D). These data indicate that SNHG3 promotes EMT by interacting with miR-326.

SNHG3 functions as a ceRNA for miR-326, promoting SMAD3 expression

By searching the TargetScan website (http://www.targetscan.org/), we found that the 3′-UTR of SMAD3 mRNA contains the sequence complementary to miR-326 (Fig. 5A). Thus, luciferase reporter assays were performed to

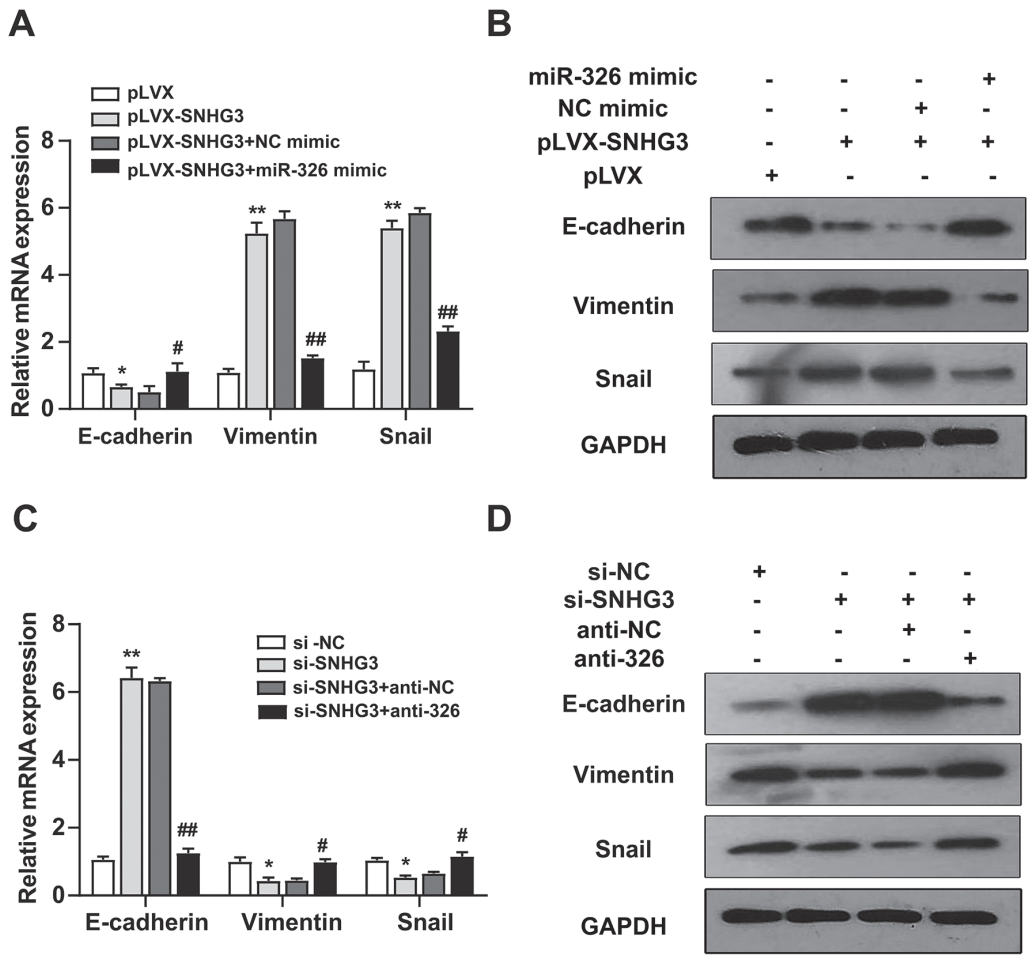

Fig. 4. SNHG3 regulates EMT process through binding with miR-326.
(A) Effects of SNHG3 on the expression levels of E-cadherin, Vimentin, and Snail mRNAs in HepG2 cells. qRT-PCR showed miR-326 mimic reversed the altered expression of E-cadherin, Vimentin, and Snail mRNAs.
*$P < 0.01$, vs. pLVX; $^{\#}P < 0.01$, vs. pLVX-SNHG3+NC mimic; **$P < 0.001$, vs. pLVX; $^{\#\#}P < 0.001$, vs. pLVX-SNHG3+NC mimic.
(B) Western blot analysis showed that miR-326 mimic reversed the altered expression of E-cadherin, Vimentin, and Snail proteins.
(C) qRT-PCR showed anti-326 reversed the altered expression of E-cadherin, Vimentin, and Snail at mRNA level in HCCLM3 cells.
*$P < 0.01$, vs. si-NC; $^{\#}P < 0.01$, vs. si-SNHG3+anti-NC; **$P < 0.001$, vs. si-NC; $^{\#\#}P < 0.001$, vs. si-SNHG3+anti-NC.
(D) Western blot showed anti-326 reversed the altered expression of E-cadherin, Vimentin, and Snail at protein level.

test whether miR-326 interacts with the 3′-UTR of SMAD3 mRNA. As predicted, the luciferase activities were significantly lower in HepG2 cells cotransfected with SMAD3-WT and miR-326 mimic than those in cells cotransfected with SMAD3-WT and NC-mimic (Fig. 5B), while no apparent effect of miR-326 mimic was detected with SMAD3-MUT. These results suggest that miR-326 may bind to 3′-UTR of SMAD3 mRNA. Subsequently, the effect of miR-326 was analyzed on the expression levels of SMAD mRNA and protein; miR-326 mimic decreased SMAD3 expression in HCCLM3 cells, whereas anti-326 increased SMAD3 expression in HepG2 cells (Fig. 5C-E). These results indicate that miR-326 reduces the expression levels of SMAD3 by interacting with its 3′-UTR.

Because SNHG3 and the 3′-UTR of SMAD3 mRNA share the same miR-326-binding sequence (Figs. 1F and 5A), we assumed that SNHG3 may modulate SMAD3 expression as a ceRNA of miR-326 in HCC. qRT-PCR was designed to investigate whether expression of SMAD3 mRNA is regulated by SNHG3. The results showed that the SMAD3 mRNA level was elevated by SNHG3 overexpression, which was reduced by miR-326 mimic (Fig. 5F). Conversely, SNHG3 knockdown decreased the SMAD3 mRNA level, which was reversed by anti-326 (Fig. 5G). These results suggest that SNHG3 may increase SMAD3 expression by interacting with miR-326.

SNHG3 promotes the progression of HCC by regulating ZEB1

It has been suggested that SMAD3 could directly bind

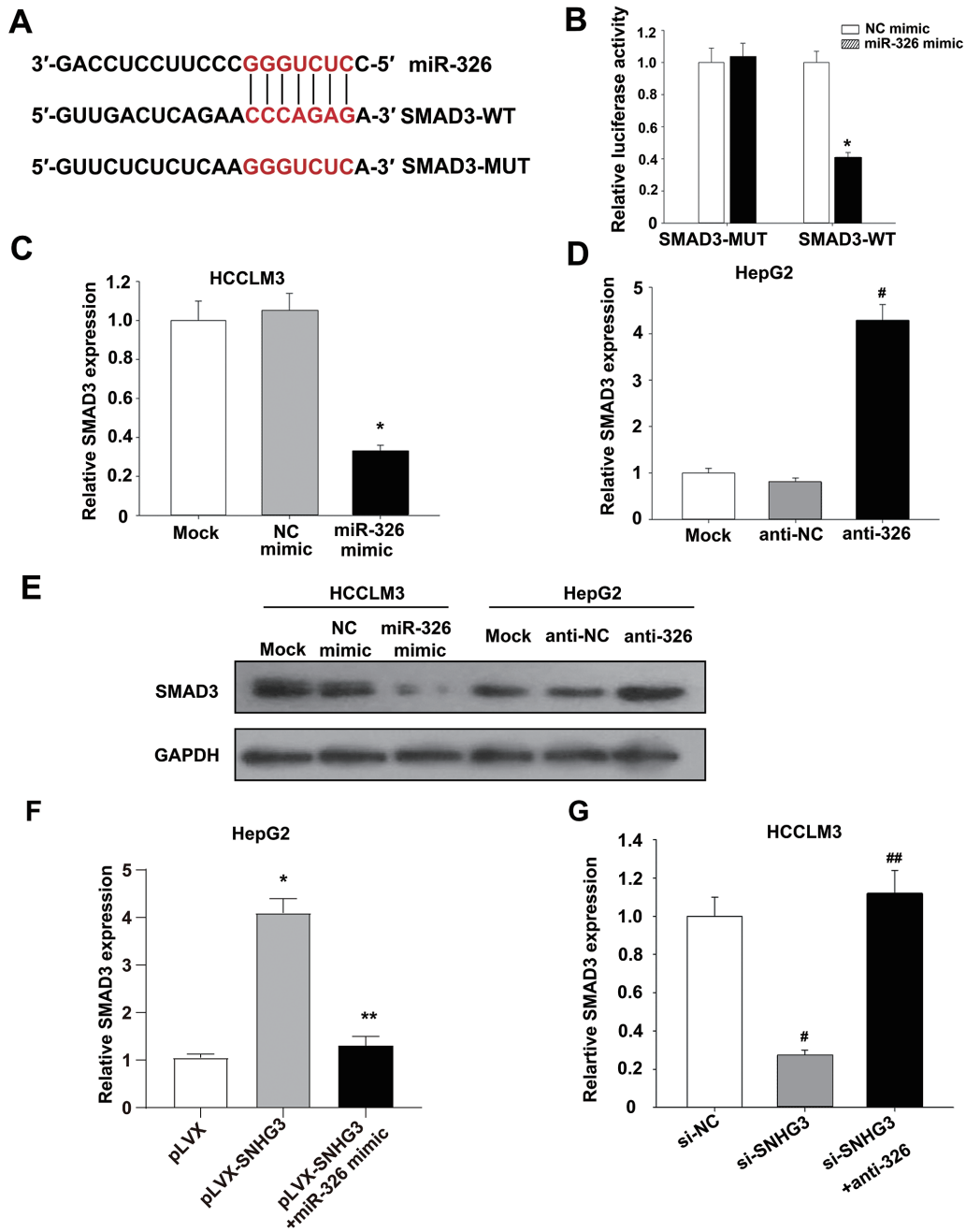

Fig. 5. SMAD3 mRNA is a target of miR-326.

(A) Potential miR-326-binding site in 3′-UTR of SMAD3 mRNA. Wild-type 3′-UTR (SMAD3-WT) and mutated 3′-UTR (SMAD3-MUT) are shown.

(B) Interaction between miR-326 and 3′-UTR of SMAD3 mRNA, judged by Luciferase reporter assays. Shown are luciferase activities in HepG2 cells cotransfected with mi-R326 mimic or NC mimic and the luciferase vector containing sequences of SMAD3 wild type or mutant type. Experiments were repeated at least 3 times; data represent mean ± SD.

*$P < 0.01$, vs. NC mimic.

(C, D) Effects of mi-R326 on the expression levels of SMAD3 mRNA. qRT-PCR analyzed mRNA levels of SMAD3 in HCCLM3 cells transfected with miR-326 mimic or NC mimic (C) and in HepG2 cells transfected with anti-326 or anti-NC (D). Experiments were repeated at least 3 times; data represent mean ± SD.

*$P < 0.01$, vs. NC mimic; $^{\#}P < 0.01$, vs. anti-NC.

(E) Western blot analyzed protein levels of SMAD3 in HCCLM3 cells transfected with miR-326 mimic or NC mimic and in HepG2 cells transfected with anti-326 or anti-NC.

(F) qRT-PCR analysis of SMAD3 mRNA levels in HepG2 cells transfected with pLVX, pLVX-SNHG3, or cotransfected with pLVX-SNHG3 and miR-326 mimic.

*$P < 0.01$, vs. pLVX; **$P < 0.01$, vs. pLVX-SNHG3.

(G) qRT-PCR analysis of SMAD3 mRNA levels in HCCLM3 cells transfected with si-NC or si-SNHG3, or cotransfected with si-SNHG3 and anti-326.

$^{\#}P < 0.01$, vs. si-NC; $^{\#\#}P < 0.01$, vs. si-SNHG3.

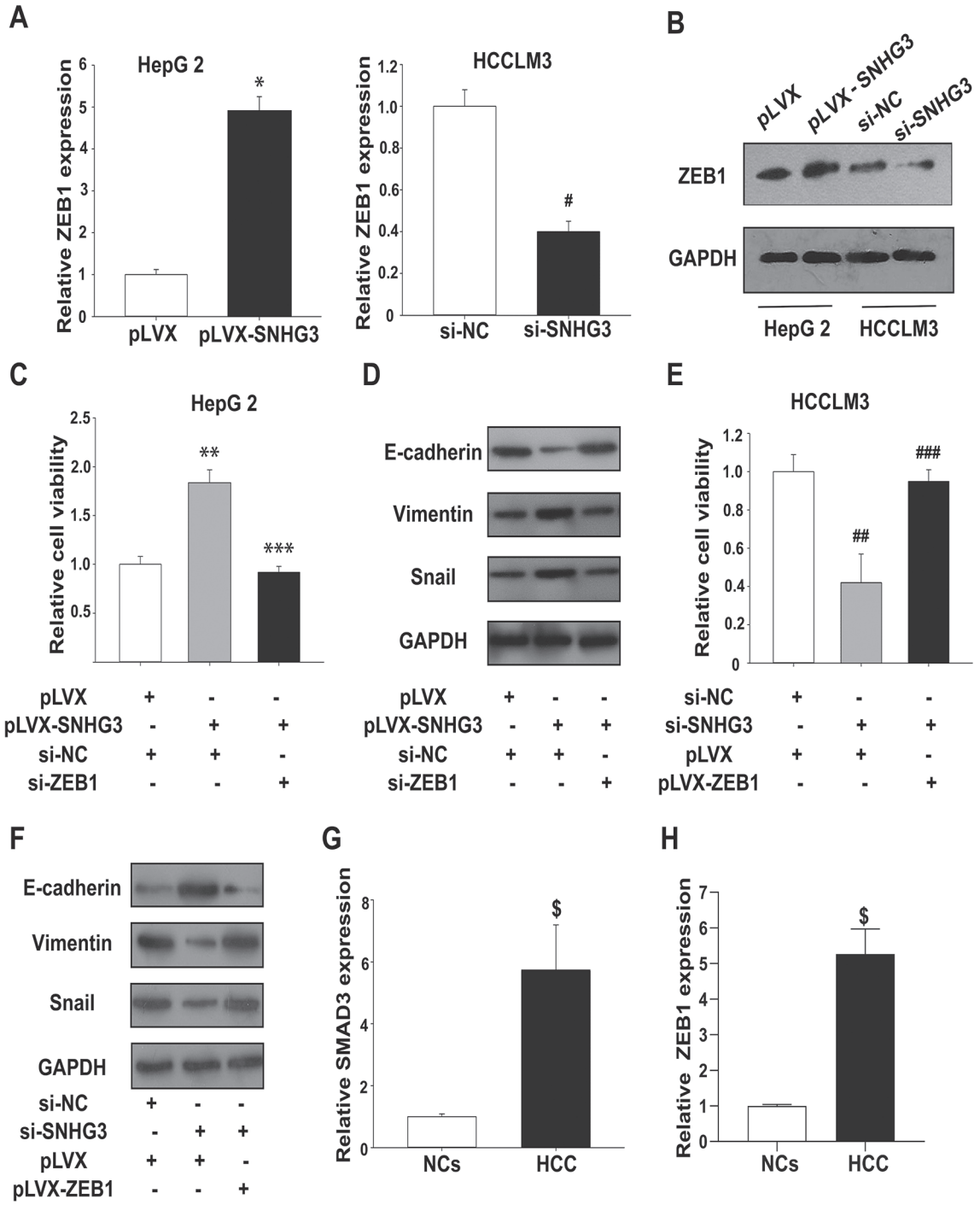

Fig. 6. SNHG3 facilitates HCC progression through ZEB1 signaling.

Experiments were repeated at least 3 times; data represent mean ± SD.

(A, B) Involvement of SNHG3 in ZEB1 expression. qRT-PCR and western blot analyses of ZEB1 expression in HepG2 cells transfected with pLVX or pLVX-SNHG3 and in HCCLM3 cells transfected with si-NC or si-SNHG3.

$^{*}P < 0.01$; $^{\#}P < 0.01$.

(C, D) Knockdown of ZEB1 expression. HepG2 cells were cotransfected with pLVX-SNHG3 and si-NC or si-ZEB1. MTT assays indicate the requirement of ZEB1 for the enhancing effects of SNHG3 on cell viability (C).

$^{**}P < 0.01$, vs. pLVX (+) + si-NC (+); $^{***}P < 0.01$, vs. pLVX-SNHG3 (+) + si-NC (+). Western blot analyses (D) showed that ZEB1 was involved in the effects of SNHG3 on expression levels of E-cadherin, Vimentin, and Snail.

(E, F) Overexpression of ZEB1 in SNHG3 functions. MTT assays (E) and Western blot analysis (F) detected the cell viability and expression of E-cadherin, Vimentin, and Snail in HCCLM3 cells transfected with si-SNHG3 or cotransfected with si-SNHG3 and pLVX-ZEB1.

$^{\#\#}P < 0.01$, vs. pLVX(+)+si-NC(+); $^{\#\#\#}P < 0.01$, vs. si-SNHG3+pLVX(+).

(G, H) Relative expression levels of SMAD3 and ZEB1 mRNAs in HCC tissues (N = 47) and matched adjacent normal, measured by qRT-PCR analysis.

$^{\$}P < 0.001$.

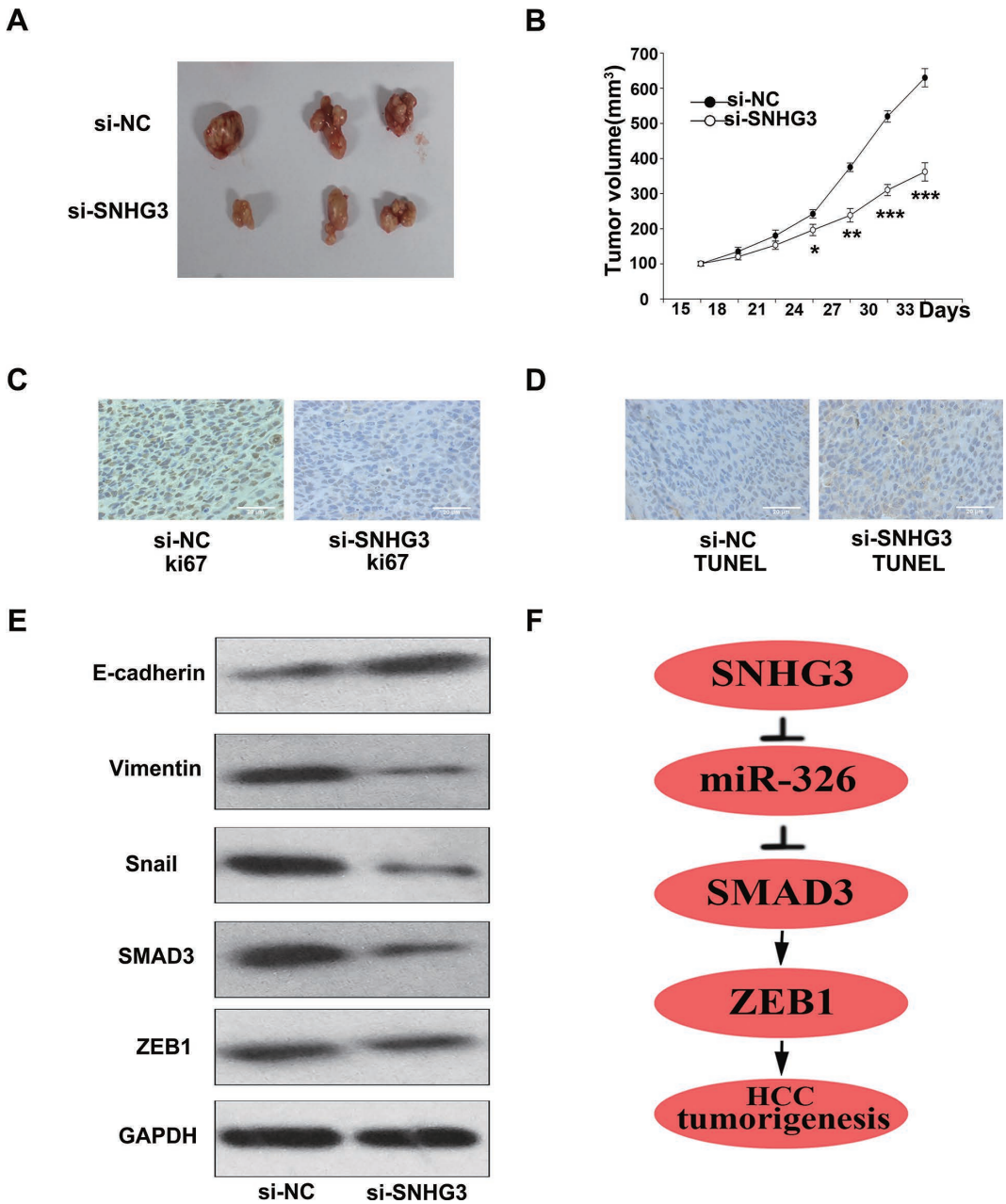

Fig. 7. SNHG3 promotes HCC cell growth through ZEB1 signaling in mice.
(A) The excised tumor tissues of grafted HepG2 cells.
(B) Tumor volumes of grafted HCC cells from days 15 to 33. Experiments were repeated at least 3 times; data represent mean ± S.D.
*$P < 0.05$, vs. si-NC; **$P < 0.01$, vs. si-NC; ***$P < 0.001$, vs. si-NC.
(C) Representative images of Ki-67 staining under microscope (× 100).
(D) Representative images of TUNEL staining under microscope (× 100).
(E) Western blot analyses of SMAD3, ZEB1, and EMT-related proteins in tumor tissues.
(F) A proposed role of SNHG3 in HCC.

to ZEB1 to activate its expression (Postigo 2003; Cao et al. 2018). We thus analyzed ZEB1 expression under the conditions of altered SNHG3 expression in HCC cells. The expression levels of ZEB1 mRNA and protein were increased by SNHG3 overexpression in HepG2 cells (Fig. 6A, B), whereas they were decreased by SNHG3 knockdown in HCCLM3 cells. These results suggest the requirement of SNHG3 for ZEB1 expression. To explore whether ZEB1 is involved in the functions of SNHG3, we knocked-down ZEB1 expression together with SNHG3 overexpression and determined the proliferation ability and EMT of HepG2 cells. The results showed that si-ZEB1 abolished the enhancing effects of SNHG3 on cell proliferation and EMT in HepG2 cells (Fig. 6C, D). We then analyzed the

effects of ZEB1 overexpression on the SNHG3 functions. In this series of experiments, HCCLM3 cells overexpressing ZEB1 were transfected with si-SNHG3 (Fig. 6E, F). ZEB1 overexpression restored the decreased cell viability and enhanced EMT process caused by SNHG3 knockdown. These results suggest that SNHG3 may accelerate HCC progression through ZEB1 signal transduction. Lastly, we confirmed that the expression levels of SMAD3 and ZEB1 mRNAs were significantly higher in human HCC tissues compared with the matched adjacent noncancerous tissues (Fig. 6G, H).

SNHG3 expression correlates with HCC progression in vivo

The role of SNHG3 in HCC tumorigenesis was then analyzed *in vivo*. SNHG3-silenced HCC cells and negative control cells were established and transplanted into mice. The results showed that SNHG3 knockdown significantly inhibited tumor growth (Fig. 7A, B) and alleviated the staining intensity of proliferating cell nuclear antigen Ki-67 (Fig. 7C). In addition, TUNEL staining demonstrated that silencing SNHG3 led to increased apoptosis (Fig. 7D). Western blot analyses indicated that SNHG3 depletion reduced SMAD3, ZEB1, vimentin, and Snai protein levels and increased E-cadherin levels (Fig. 7E).

Taken together, we propose that SNHG3 promotes HCC progression by reducing the expression level of miR-326, which in turn activates the SMAD3/ZEB1 signaling pathway (Fig. 7F).

Discussion

Many studies have verified that lncRNAs play vital roles in the pathogenesis of HCC (Deng et al. 2015; Li et al. 2015a; Sui et al. 2016). However, the functions and mechanisms of SNHG3 in HCC remain unclear. We demonstrated that SNHG3 expression in HCC tissues was significantly increased compared with corresponding adjacent noncancerou tissues and was correlated with the TNM stage of patients with HCC (Table 1). It has been reported that multiple lncRNAs in the SNHG family, such as SNHG1 and SNHG5, can sponge miRNAs to regulate their expression in different cancers, including prostate cancer and gastric cancer, thus participating in the tumor growth (Li et al. 2017; Zhao et al. 2017). In addition, miR-326 has been demonstrated to inhibit the growth of various types of tumors including HCC (Kim et al. 2014; Li et al. 2015b; Cao et al. 2016; Wu et al. 2017; Zhang et al. 2017; Yin et al. 2018). However, the relationship between SNHG3 and miR-326 in HCC remains unclear. In this study, miR-326 levels were lower in HCC tissues, and the expression of miR-326 showed an opposite trend with SNHG3 expression in HCC tissues (Fig. 1).

SNHG3 contains a miR-326-binding sequence, and the dual-luciferase reporter assay suggests the interaction between miR-326 and SNHG3 (Fig. 1). In addition, SNHG3 overexpression significantly enhanced proliferation, migration, and EMT processes but reduced the apoptosis rate in HepG2 cells. By contrast, knockdown of SNHG3 significantly decreased proliferation, migration, and EMT but promoted apoptosis in HCCLM3 cells. Importantly, these effects were reversed by miR-326 mimic or anti-326, respectively (Figs. 2, 3 and 4), indicating that SNHG3 could exert oncogenic functions by regulating miR-326 in HCC.

SMAD3, a highly active and ubiquitous transcription factor, is responsible for stimulating the transcription of various target genes, thereby participating in the characteristic manifestation of malignant tumors, including HCC (Yang et al. 2006). Indeed, the high level of SMAD3 is confirmed to be related to the poor prognosis in HCC (Zhang et al. 2016; Zhang et al. 2019). In this study, we demonstrated that miR-326 could reduce SMAD3 expression, whereas anti-326 could increase SMAD3 expression. Moreover, SNHG3 overexpression increased the level of SMAD3 mRNA, which could be reversed by miR-326 mimic. Conversely, SNHG3 knockdown reduced level of SMAD3 mRNA, which was reversed by anti-326 (Fig. 5). These results indicate that SNHG3 modulates SMAD3 expression by interacting with miR-326.

As a member of the zinc finger protein family, ZEB1 was identified as a necessary mediator of cancer metastasis, including HCC (Bai et al. 2014; Wang et al. 2014b). Moreover, ZEB1 exerted oncogenic functions, including promoting survival, proliferation, migration, invasion, and the EMT phenotype of tumor cells and preventing tumor cell apoptosis (Lee et al. 2014; Sanchez-Tillo et al. 2015; Yun et al. 2015; Chang et al. 2016). SMAD3 could directly bind to ZEB1 to induce its expression (Postigo 2003; Cao et al. 2018). To assess whether SNHG3 could regulate HCC activities through SMAD3/ZEB1 signaling, we measured ZEB1 expression in HCC cells after altering SNHG3 expression. The results showed that SNHG3 overexpression significantly increased ZEB1 expression, whereas SNHG3 silencing reduced ZEB1 expression. We also observed that silencing ZEB1 inhibited the SNHG3 overexpression-mediated effects on proliferation and EMT processes in HepG2 cells (Fig. 6C, D). Importantly, the expression levels of SMAD3 and ZEB1 were significantly higher in HCC tissues compared with adjacent noncancerous tissues (see Fig. 6G, H). Taken together, we propose that SNHG3 could promote HCC progression by activating SMAD3/ZEB1 signaling.

Acknowledgments

This study was supported by the Key Project of Chinese Ministry of Science and Technology (2018ZX10301406 and 2017ZX10202202), the National Natural Science Foundation of China (81600494), and the Natural Science Foundation of Shandong Province (ZR2016HQ42).

Conflict of Interest

The authors declare no conflict of interest.

References

Ahn, S.M., Cha, J.Y., Kim, J., Kim, D., Trang, H.T., Kim, Y.M., Cho, Y.H., Park, D. & Hong, S. (2012) Smad3 regulates E-cadherin via miRNA-200 pathway. *Oncogene*, **31**, 3051-3059.

Bai, W.D., Ye, X.M., Zhang, M.Y., Zhu, H.Y., Xi, W.J., Huang, X., Zhao, J., Gu, B., Zheng, G.X., Yang, A.G. & Jia, L.T. (2014) MiR-200c suppresses TGF-beta signaling and counteracts trastuzumab resistance and metastasis by targeting ZNF217 and ZEB1 in breast cancer. *Int. J. Cancer*, **135**, 1356-1368.

Cao, L., Wang, J. & Wang, P.Q. (2016) MiR-326 is a diagnostic biomarker and regulates cell survival and apoptosis by targeting Bcl-2 in osteosarcoma. *Biomed. Pharmacother.*, **84**, 828-835.

Cao, Y., Liu, Y., Ping, F., Yi, L., Zeng, Z. & Li, Y. (2018) miR-200b/c attenuates lipopolysaccharide-induced early pulmonary fibrosis by targeting ZEB1/2 via p38 MAPK and TGF-beta/smad3 signaling pathways. *Lab. Invest.*, **98**, 339-359.

Chang, L., Yuan, Y., Li, C., Guo, T., Qi, H., Xiao, Y., Dong, X., Liu, Z. & Liu, Q. (2016) Upregulation of SNHG6 regulates ZEB1 expression by competitively binding miR-101-3p and interacting with UPF1 in hepatocellular carcinoma. *Cancer Lett.*, **383**, 183-194.

Chang, S., Chen, B., Wang, X., Wu, K. & Sun, Y. (2017) Long non-coding RNA XIST regulates PTEN expression by sponging miR-181a and promotes hepatocellular carcinoma progression. *BMC Cancer*, **17**, 248.

Deng, L., Yang, S.B., Xu, F.F. & Zhang, J.H. (2015) Long noncoding RNA CCAT1 promotes hepatocellular carcinoma progression by functioning as let-7 sponge. *J. Exp. Clin. Cancer Res.*, **34**, 18.

Esteller, M. (2011) Non-coding RNAs in human disease. *Nat. Rev. Genet.*, **12**, 861-874.

Fei, F., He, Y., He, S., He, Z., Wang, Y., Wu, G. & Li, M. (2018) LncRNA SNHG3 enhances the malignant progress of glioma through silencing KLF2 and p21. *Biosci. Rep.*, **38**, pii: BSR20180420.

Forner, A., Llovet, J.M. & Bruix, J. (2012) Hepatocellular carcinoma. *Lancet*, **379**, 1245-1255.

Ge, Y., Yan, X., Jin, Y., Yang, X., Yu, X., Zhou, L., Han, S., Yuan, Q. & Yang, M. (2015) MiRNA-192 [corrected] and miRNA-204 directly suppress lncRNA HOTTIP and interrupt GLS1-mediated glutaminolysis in hepatocellular carcinoma. *PLoS Genet.*, **11**, e1005726.

Hong, L., Chen, W., Wu, D. & Wang, Y. (2018) Upregulation of SNHG3 expression associated with poor prognosis and enhances malignant progression of ovarian cancer. *Cancer Biomark.*, **22**, 367-374.

Huang, F.T., Chen, W.Y., Gu, Z.Q., Zhuang, Y.Y., Li, C.Q., Wang, L.Y., Peng, J.F., Zhu, Z., Luo, X., Li, Y.H., Yao, H.R. & Zhang, S.N. (2017a) The novel long intergenic noncoding RNA UCC promotes colorectal cancer progression by sponging miR-143. *Cell Death Dis.*, **8**, e2778.

Huang, J.L., Cao, S.W., Ou, Q.S., Yang, B., Zheng, S.H., Tang, J., Chen, J., Hu, Y.W., Zheng, L. & Wang, Q. (2018) The long non-coding RNA PTTG3P promotes cell growth and metastasis via up-regulating PTTG1 and activating PI3K/AKT signaling in hepatocellular carcinoma. *Mol. Cancer*, **17**, 93.

Huang, S.K., Li, Y., Yuan, X.H., Zhao, M., Wang, J., Li, Y., Li, Y., Lin, H., Zhang, Q., Wang, W.J., Li, D.D., Dong, X., Li, L.F., Liu, M., Huang, W.Y., et al. (2019) The UbL-UBA Ubiquilin4 protein functions as a tumor suppressor in gastric cancer by p53-dependent and p53-independent regulation of p21. *Cell Death Differ.*, **26**, 516-530.

Huang, W., Tian, Y., Dong, S., Cha, Y., Li, J., Guo, X. & Yuan, X. (2017b) The long non-coding RNA SNHG3 functions as a competing endogenous RNA to promote malignant development of colorectal cancer. *Oncol. Rep.*, **38**, 1402-1410.

Kim, Y., Kim, H., Park, H., Park, D., Lee, H., Lee, Y.S., Choe, J., Kim, Y.M. & Jeoung, D. (2014) miR-326-histone deacetylase-3 feedback loop regulates the invasion and tumorigenic and angiogenic response to anti-cancer drugs. *J. Biol. Chem.*, **289**, 28019-28039.

Lazarova, D. & Bordonaro, M. (2017) ZEB1 mediates drug resistance and EMT in p300-deficient CRC. *J. Cancer*, **8**, 1453-1459.

Lee, J.Y., Park, M.K., Park, J.H., Lee, H.J., Shin, D.H., Kang, Y., Lee, C.H. & Kong, G. (2014) Loss of the polycomb protein Mel-18 enhances the epithelial-mesenchymal transition by ZEB1 and ZEB2 expression through the downregulation of miR-205 in breast cancer. *Oncogene*, **33**, 1325-1335.

Li, J., Zhang, Z., Xiong, L., Guo, C., Jiang, T., Zeng, L., Li, G. & Wang, J. (2017) SNHG1 lncRNA negatively regulates miR-199a-3p to enhance CDK7 expression and promote cell proliferation in prostate cancer. *Biochem. Biophys. Res. Commun.*, **487**, 146-152.

Li, T., Xie, J., Shen, C., Cheng, D., Shi, Y., Wu, Z., Deng, X., Chen, H., Shen, B., Peng, C., Li, H., Zhan, Q. & Zhu, Z. (2015a) Amplification of long noncoding RNA ZFAS1 promotes metastasis in hepatocellular carcinoma. *Cancer Res.*, **75**, 3181-3191.

Li, Y., Gao, Y., Xu, Y., Ma, H. & Yang, M. (2015b) Down-regulation of miR-326 is associated with poor prognosis and promotes growth and metastasis by targeting FSCN1 in gastric cancer. *Growth Factors*, **33**, 267-274.

Liu, L., Ni, J. & He, X. (2018) Upregulation of the long noncoding RNA SNHG3 promotes lung adenocarcinoma proliferation. *Dis. Markers*, **2018**, 5736716.

Lu, W., Yu, J., Shi, F., Zhang, J., Huang, R., Yin, S., Songyang, Z. & Huang, J. (2019) The long non-coding RNA Snhg3 is essential for mouse embryonic stem cell self-renewal and pluripotency. *Stem Cell. Res. Ther.*, **10**, 157.

Lu, W., Zhang, H., Niu, Y., Wu, Y., Sun, W., Li, H., Kong, J., Ding, K., Shen, H.M., Wu, H., Xia, D. & Wu, Y. (2017) Long non-coding RNA linc00673 regulated non-small cell lung cancer proliferation, migration, invasion and epithelial mesenchymal transition by sponging miR-150-5p. *Mol. Cancer*, **16**, 118.

Maluccio, M. & Covey, A. (2012) Recent progress in understanding, diagnosing, and treating hepatocellular carcinoma. *CA Cancer J. Clin.*, **62**, 394-399.

Nagano, T. & Fraser, P. (2011) No-nonsense functions for long noncoding RNAs. *Cell*, **145**, 178-181.

Pelczar, P. & Filipowicz, W. (1998) The host gene for intronic U17 small nucleolar RNAs in mammals has no protein-coding potential and is a member of the 5′-terminal oligopyrimidine gene family. *Mol. Cell. Biol.*, **18**, 4509-4518.

Ponting, C.P., Oliver, P.L. & Reik, W. (2009) Evolution and functions of long noncoding RNAs. *Cell*, **136**, 629-641.

Postigo, A.A. (2003) Opposing functions of ZEB proteins in the regulation of the TGFbeta/BMP signaling pathway. *EMBO J.*, **22**, 2443-2452.

Salmena, L., Poliseno, L., Tay, Y., Kats, L. & Pandolfi, P.P. (2011) A ceRNA hypothesis: the Rosetta Stone of a hidden RNA language? *Cell*, **146**, 353-358.

Sanchez-Tillo, E., de Barrios, O., Valls, E., Darling, D.S., Castells, A. & Postigo, A. (2015) ZEB1 and TCF4 reciprocally modulate their transcriptional activities to regulate Wnt target gene expression. *Oncogene*, **34**, 5760-5770.

Sui, C.J., Zhou, Y.M., Shen, W.F., Dai, B.H., Lu, J.J., Zhang, M.F. & Yang, J.M. (2016) Long noncoding RNA GIHCG promotes hepatocellular carcinoma progression through epigenetically regulating miR-200b/a/429. *J. Mol. Med.* (*Berl.*), **94**, 1281-1296.

Torre, L.A., Bray, F., Siegel, R.L., Ferlay, J., Lortet-Tieulent, J. & Jemal, A. (2015) Global cancer statistics, 2012. *CA Cancer J. Clin.*, **65**, 87-108.

Wang, F., Yuan, J.H., Wang, S.B., Yang, F., Yuan, S.X., Ye, C., Yang, N., Zhou, W.P., Li, W.L., Li, W. & Sun, S.H. (2014a) Oncofetal long noncoding RNA PVT1 promotes proliferation and stem cell-like property of hepatocellular carcinoma cells by stabilizing NOP2. *Hepatology*, **60**, 1278-1290.

Wang, Y., He, L., Du, Y., Zhu, P., Huang, G., Luo, J., Yan, X., Ye, B., Li, C., Xia, P., Zhang, G., Tian, Y., Chen, R. & Fan, Z. (2015) The long noncoding RNA lncTCF7 promotes self-renewal of human liver cancer stem cells through activation of Wnt signaling. *Cell Stem Cell*, **16**, 413-425.

Wang, Y., Wen, M., Kwon, Y., Xu, Y., Liu, Y., Zhang, P., He, X., Wang, Q., Huang, Y., Jen, K.Y., LaBarge, M.A., You, L., Kogan, S.C., Gray, J.W., Mao, J.H., et al. (2014b) CUL4A induces epithelial-mesenchymal transition and promotes cancer metastasis by regulating ZEB1 expression. *Cancer Res.*, **74**, 520-531.

Wen, X., Yao, M., Lu, Y., Chen, J., Zhou, J., Chen, X., Zhang, Y., Lu, W., Qian, X., Zhao, J., Zhang, L., Ding, S. & Lu, F. (2018) Integration of prealbumin into child-pugh classification improves prognosis predicting accuracy in HCC patients considering curative surgery. *J. Clin. Transl. Hepatol.*, **6**, 377-384.

Wu, X., Cao, X. & Chen, F. (2017) WITHDRAWN: LncRNA-HOTAIR activates tumor cell proliferation and migration by suppressing MiR-326 in cervical cancer. *Oncol. Res*., doi: 10.3727/096504017X15037515496840 [Epub ahead of print].

Yang, Y.A., Zhang, G.M., Feigenbaum, L. & Zhang, Y.E. (2006) Smad3 reduces susceptibility to hepatocarcinoma by sensitizing hepatocytes to apoptosis through downregulation of Bcl-2. *Cancer Cell*, **9**, 445-457.

Yao, Z., Xiong, Z., Li, R., Liang, H., Jia, C. & Deng, M. (2018) Long non-coding RNA NRON is downregulated in HCC and suppresses tumour cell proliferation and metastasis. *Biomed. Pharmacother.*, **104**, 102-109.

Yin, S., Du, W., Wang, F., Han, B., Cui, Y., Yang, D., Chen, H., Liu, D., Liu, X., Zhai, X. & Jiang, C. (2018) MicroRNA-326 sensitizes human glioblastoma cells to curcumin via the SHH/GLI1 signaling pathway. *Cancer Biol. Ther.*, **19**, 260-270.

Yuan, J.H., Yang, F., Wang, F., Ma, J.Z., Guo, Y.J., Tao, Q.F., Liu, F., Pan, W., Wang, T.T., Zhou, C.C., Wang, S.B., Wang, Y.Z., Yang, Y., Yang, N., Zhou, W.P., et al. (2014) A long noncoding RNA activated by TGF-beta promotes the invasion-metastasis cascade in hepatocellular carcinoma. *Cancer Cell*, **25**, 666-681.

Yun, E.J., Baek, S.T., Xie, D., Tseng, S.F., Dobin, T., Hernandez, E., Zhou, J., Zhang, L., Yang, J., Sun, H., Xiao, G., He, D., Kittler, R. & Hsieh, J.T. (2015) DAB2IP regulates cancer stem cell phenotypes through modulating stem cell factor receptor and ZEB1. *Oncogene*, **34**, 2741-2752.

Zhang, P., Kong, F., Deng, X., Yu, Y., Hou, C., Liang, T. & Zhu, L. (2017) MicroRNA-326 suppresses the proliferation, migration and invasion of cervical cancer cells by targeting ELK1. *Oncol. Lett.*, **13**, 2949-2956.

Zhang, P.F., Wang, F., Wu, J., Wu, Y., Huang, W., Liu, D., Huang, X.Y., Zhang, X.M. & Ke, A.W. (2019) LncRNA SNHG3 induces EMT and sorafenib resistance by modulating the miR-128/CD151 pathway in hepatocellular carcinoma. *J. Cell. Physiol.*, **234**, 2788-2794.

Zhang, T., Cao, C., Wu, D. & Liu, L. (2016) SNHG3 correlates with malignant status and poor prognosis in hepatocellular carcinoma. *Tumour Biol.*, **37**, 2379-2385.

Zhao, L., Han, T., Li, Y., Sun, J., Zhang, S., Liu, Y., Shan, B., Zheng, D. & Shi, J. (2017) The lncRNA SNHG5/miR-32 axis regulates gastric cancer cell proliferation and migration by targeting KLF4. *FASEB J.*, **31**, 893-903.